Dynamic wind farm power simulation

Dougal McQueen, Alan Wood, and Allan Miller
Electric Power Engineering Centre, University of Canterbury, NEW ZEALAND.
Email: dougal.mcqueen@pg.canterbury.ac.nz

***Abstract*—Wind energy represents one of the least cost methods of electricity generation, produces no carbon emissions, and is highly scaleable. However, the intermittency of wind and the passive reaction of wind turbines means spinning and scheduled reserves are required to ensure grid security. It is vital for transmission network planning that temporally and spatially accurate models of wind power are formulated. While there are many approaches to the simulation of wind speed time-series there is less information available to aid in characterising the dynamic transformation from wind speed time-series to wind power time-series. Wind farms comprise arrays of wind turbines, and individual wind turbines have well defined power curves, however the aggregation of the individual wind turbine power time-series is not independent; thus a temporally consistent model for the spatial correlation of the wind resource is required. Measurements made at a wind farm in New Zealand are used to construct two models and simulations compared with measured power. The first applies the Sandia method coupled with the convolution of a Gaussian function and the wind turbine power curve. The second method uses the Measure Correlate Predict (MCP) methodology and Wavelet Multi-resolution Analysis (WMA). The MCP / WMA model is then applied to generate wind farm power curves for farms of differing topographies, and a simple model comprising Gaussian smoothing and a first order low pass filter matched to the results.**

I. INTRODUCTION

To enable greater penetration of wind energy into electricity networks it is essential good time-series models for wind power are developed. It is possible to use historic measurements, or meteorological model outputs, to develop coherent sets of wind speed time-series that are representative of envisaged wind farms [1]. These wind speed time-series must be transformed to the corresponding wind power time-series. For the wind power time-series to be truly representative of the wind farms the transform must be accurate for both the steady-state and dynamic characteristics.

The transformation from wind speed to power by an individual wind turbine is well characterised by the wind turbine power curve which is often calibrated using IEC-61400-12 [2]. For example; the wind turbine power curve for the Gamesa G52 turbine, used in analyses in this paper, has been obtained from sales documentation [3]. However, a wind farm comprises a group of spatially distributed wind turbines, and the wind farm power curve is more enigmatic. The wind turbines are spaced apart so turbines do not suffer undue fatigue due to turbulence induced in turbine wakes, and capture the maximum amount of energy. The terrain is not always uniform, thus each turbine will experience different magnitudes of wind speed. This spread of wind speeds can be modeled, as a steady state function, by smoothing the wind turbine power curve [4].

Further, the winds incident on wind turbines are not independent; turbines in close proximity fetch similar wind hence produce more strongly correlated power than turbines farther apart. This behaviour is the result of turbulence which is dependent upon the distance between turbines and the time-scale. The reaction of the wind turbines to turbulence defines the dynamic character of the produced power.

Data from the Mt Stuart wind farm are used to develop and apply models for simulating wind power. Measurements made at the meteorological mast are used to provide a reference wind speed and direction time-series. This time-series is modified using three methods to provide a wind farm power time-series. The modification involves modeling the steady state and dynamic behaviours. The three methods for modeling the steady state are; a Gaussian filter, Measure Correlate Predict (MCP), and a Gaussian Speed-Up (GSU) model. The three methods for simulating the dynamic response are; the Sandia method, a Wavelet multi-Resolution Analysis (WMA) approach, and a first order low pass filter (LPF).

The simulated power time-series are multiplied by a Markov chain model, derived from the operational data, to account for operational efficiency (as is applied by Sulaeman [5]). The resultant power time-series are compared with measurements made at the Mt Stuart wind farm.

The MCP / WMA method is subsequently used to produce power time series representative of wind farms of differing topographies, and the GSU / LPF model fitted to these simulations so that characteristics resulting from the differing topographies can be examined.

II. MT STUART WIND FARM

The Mt Stuart Wind Farm comprises nine $850\,\text{kW}$ Gamesa G52 wind turbines (total $7.65\,\text{MW}$) with a hub height of 45 meters, stretching north to south in a single line across the top of Mt Stuart. Mt Stuart is in South Otago, New Zealand, and is elevated above the rolling hill country, well exposed to the prevailing westerly winds. Each wind turbine has a cup anemometer mounted on the rear of the nacelle. The wind farm also has a 30 meter meteorological mast, sited between turbines, near the middle of the wind farm. Power, wind speed, and nacelle orientation for each turbine, as well as total wind farm power, and meteorological mast wind speed and direction data have been extracted from the SCADA, at a temporal resolution of 1 min, for a period of one year.

The wind speed time-series derived from the nacelle anemometers have a high pass filter applied to assist in turbine fault diagnostics. Further the nacelle aneometers are located behind the turbine rotor and thus affected by the rotor wake and the nacelle. It is therefore necessary to scale the nacelle wind speed time-series such that they are representative of the free stream wind speed. Kolmogorov's theory for

the spectral energy density, as presented in Equation 1, is used as a target to scale the nacelle wind speed time-series.

$$E(k) = C\epsilon^{\frac{2}{3}}k^{\frac{-5}{3}} \quad (1)$$

Where E is the energy density, k is the wave number, C is a universal constant, and ϵ is the eddy viscosity.

The wind speed across Mt Stuart varies according to the boundary layer stability, topography, wind direction (which determines the topographic speed up), and turbulence. As the size of a wind farm is relatively small (compared with the atmosphere), the turbine and mast heights similar, and the wind farm located high on an exposed ridge with predominantly neutral stratification, changes in the boundary layer stability can be ignored [6].

III. Gaussian filter / Sandia

The first method used for modelling the transformation of wind speed to power uses a Gaussian filter for characterizing the steady state and the Sandia method to account for the dynamic response.

A. Gaussian filter

The wind speed time-series can be converted to wind power using a wind farm power curve, which accounts for diversity in topographic speed ups. The wind farm power curve is calculated by convolution of a Gaussian function with the wind turbine power curve, as described in Equation 2. The Gaussian filter approach was substantiated by De Tomassi et al. using empirical data [7] and the filter width is set to the value for a wind farm comprising 10 turbines $\sigma_{10} = 1.9196$.

$$P_g(u) = P(u) * \frac{1}{\sqrt{2\pi}\sigma_g} e^{-\frac{u^2}{2\sigma_g^2}} \quad (2)$$

Where P is power u is wind speed, g denotes the Gaussian distribution,$*$ is the convolution operator, and σ is the standard deviation or filter width.

B. Sandia method

Wind speed time-series are often generated for grids of points to support turbine load calculations. The Sandia method uses the coherence between points in the grid to modify randomly generated time-series that have a defined spectra [8]. The coherence between points can be modeled as a function of distance, frequency, and mean wind speed, as defined by Davenport, and presented in Equation 3 [9].

$$\Gamma(f, r, \bar{u}) = e^{-d\frac{r}{\bar{u}}f} \quad (3)$$

Where Γ is the coherence, f is frequency, r is separation distance, d is the decay constant, and $\bar{u}$ is the mean wind speed.

The Sandia method simulates the turbulent component of wind speed, resulting in a stationary Gaussian process, however wind speed time-series are necessarily positive and typically conform to a Weibull probability distribution. To ensure the simulated time-series are truly representative of wind speed time-series the low frequency components of the power spectra are substituted with the measured spectra from the meteorological mast (equivalent to the method described by Rose and Apt [10]). The definition of the low frequency cut-off is a trade-off between finding the frequency below which the set of wind speed times series can be considered concomitant, and the frequency above which the spectral components are not integral to the definition of the time-series shape. To ensure this method is comparable with methods employed later in this paper the cut-off is selected to be the frequency corresponding to a period of 96 minutes.

C. Simulation using Gaussian filter / Sandia method

Wind farm power time series can be simulated using the Gaussian filter / Sandia method by the following procedure:

1) White noise time-series, of a suitable length, are generated and the power spectra found by applying Fourier transforms. The power spectra are weighted to Kolmogorov's spectra (as defined in Equation 1).
2) Coherence matrices are defined for each frequency using Davenport's relationship, and the distance between each turbine pair. A decay constant of 7 is applied; representative of low coherence, or complex terrain, as suggested by Nanahara et al. [11]. The set of complex power spectra are multiplied by the Cholesky decompositions of the coherence matrices to obtain a set of correlated power spectra.
3) The low frequency components of the power spectra are substituted with the power spectra obtained from the meteorological mast.
4) Inverse Fourier transforms are applied to the resultant power spectra and time-series representative of the wind speed incident at each wind turbine found. Note that the wind speed time-series measured at the meteorological (met) mast is not measured at the turbine hub-height; hence, the met mast wind speed time-series is scaled according to the mean "speed up" as defined in Section entitled MCP.
5) Wind turbine power time-series are found by convolution with the Gaussian filter.
6) The wind farm power is the aggregate of the wind turbine power time-series.

The Sandia / Gaussian filter method characterises the spatial integration over a wind farm. However, the inertia and spatial integration of a wind turbine is not accounted for. The averaging of a wind turbine should be evident as differences in power spectral densities (PSD) of the measured wind turbine power and that simulated. However, the use of the Kolmogorov spectrum as a target for filtering nacelle wind speeds removes veracity of the simulated spectra and results here show no substantial difference between simulated and measured spectra. While it is intuitive that the wind turbine PSD should differ from that measured using cup anemometers it should be remembered that wind turbines are mechanically complex experiencing phenomena such as blade / tower interactions, thus are not representative of free stream measurements.

IV. Measure Correlate Predict / Wavelet Multi-resolution Analysis

While the Gaussian filter / Sandia method provides reasonable estimates for wind power time-series (see Results

section) the Gaussian filter is not sufficiently manipulable to be able to characterise power time-series for wind farms of varying topographies. Further the Sandia method assumes turbulence is a homoskedastic process, and while this may be acceptable for turbine load calculations it leads to underestimation of ramp rates when applied to the dynamic simulation of wind farm power across a wide range of wind speeds. Hence a method using MCP, to account for steady state factors, and WMA, to account for turbulence, is developed here.

A. MCP

Typically the relative wind speed between two points for a given wind direction is well approximated by a linear regression. Using this characteristic a methodology has been described by Derrick termed MCP [12]. In the application here for each turbine the wind speed time-series at the meteorological mast and the nacelle wind speed time-series are binned into twelve 30 degree sectors (according to the wind direction at the meteorological mast). Wind speeds less than $3ms^{-1}$ are excluded (those below turbine cut-in), and a single parameter linear regression formed by forcing the regression through the origin. The resulting slope is termed the "speed up". The speed ups can be applied to the wind speed time-series measured at the meteorological mast and hence wind speed time-series for each turbine obtained. The turbine wind speed time-series can be transformed to power using the wind turbine power curve and the aggregate of these gives the wind farm power time-series. A wind farm power curve can then be determined using the method of bins [13],and referenced to the meteorological mast wind speed as expressed in Equation 4.

$$P_S(u) = \frac{1}{12T}\sum_{t=1}^{T}\sum_{\theta=1}^{12} P(u \cdot S_{t,\theta}) \tag{4}$$

Where S is the speed up, t is the turbine index with a total of T turbines, and θ is the wind direction sector.

B. WMA

Turbulence is the result of the progression of eddies or vortices of varying sizes past a measurement point. The physical size of the eddies determines both the spatial extent and the temporal duration of their influence. Thus it is intuitive to decompose a time-series into a form whereby the influence of small scale eddies, that have local influence, are isolated from the large scale eddies, that have greater influence. Further, techniques such as Davenport's, reliant upon the Fourier expansion, (in which a time-series may be represented solely in the frequency domain), retain no information as to when in time a particular vortex transgresses and hence assume homoskedasticity.

Wavelet decomposition allows a time-series to be represented in the time-frequency plane using a dyadic structure. A wavelet is a compactly supported oscillatory function that is square integrable as presented in Equation 5. The decomposition at each scale is achieved by deconvolving the wavelet across the time-series, resulting in a wavelet coefficient series and a residual time-series, as presented in Equation 6. The wavelet series and residual time-series have a temporal resolution half that of the initial time-series. The residual time-series can be recursively decomposed by dilating the wavelet (by an order of two to ensure a dyadic structure), and deconvolving to obtain further wavelet coefficient series and residual time-series. The wavelet decomposition is achieved using the tools in the WaveLab toolbox for Matlab [14].

$$\{\psi_{j,\tau}(t) = \frac{1}{\sqrt{2^j}}\psi\left(\frac{t-2^j\tau}{2^j}\right)\}_{(j,\tau)inZ^2} \tag{5}$$

Where ψ is the mother wavelet, j is the scale, and τ is the translation.

$$\langle u(\tau, 2^j), \Psi(j,\tau)\rangle = \int_{-\infty}^{\infty} u(t)\frac{1}{\sqrt{j}}\psi^*\left(\frac{t-\tau}{j}\right)dt \tag{6}$$

Where Ψ is the wavelet coefficient series, t is time, and * denotes the complex conjugate.

The wavelet decomposition results in a number of wavelet series and a residual time-series. Each of the wavelet series can be characterised as a Auto-Regressive Moving-Average (AR-MA) process. However, the decomposition effectively increases the dimensionality of the set of time-series; the set of wavelet series having auto-correlations (see Equation 7), correlations between the wavelet series resulting from different time-series at the same scale (see Equation 8), and cross-correlation between wavelet series of adjacent scales in the same time-series (see Equation 9). To make simulation tractable it is necessary to reduce the dimensionality through careful selection of the wavelet (or quadrature mirror filter (QMF)). A variety of wavelets have been tested and it is found the Beylkin wavelet minimises the cross-correlation most effectively.

$$R(\Psi_n(j,\tau), \Psi_n(j,\tau+\delta)) = \sum_{\tau=1}^{T}\{(\Psi_n(j,\tau) - \overline{\Psi_n(j,\tau)}) \\ (\Psi_n(j,\tau+\delta) - \overline{\Psi_n(j,\tau+\delta)})\} \tag{7}$$

Where R is the Pearson's correlation coefficient, n is a measurement, and $\Psi_n(j,\tau)$ is the temporal average of the wavelet coefficients.

$$R(\Psi_n(j), \Psi_m(j)) = \sum_{\tau=1}^{T}\{(\Psi_n(j,\tau) - \overline{\Psi_n(j,\tau)}) \\ (\Psi_m(j,\tau) - \overline{\Psi_m(j,\tau)})\} \tag{8}$$

Where m is a second measurement.

$$R(\Psi_n(j), \Psi_n(j+1)) = \sum_{\delta=[-\frac{1}{4},\frac{1}{4}]}\sum_{\tau=1}^{T}\{(\Psi_n(j,\tau) - \overline{\Psi_n(j,\tau)}) \\ (\Psi_n(j+1,\tau+\delta) - \overline{\Psi_n(j+1,\tau+\delta)})\} \tag{9}$$

To support the methods here the time-series should be decomposed such that the wavelet coefficient series characterise turbulence and the residual time-series represents the weather forcing. This can be identified by defining the terminal stage of decomposition to be the scale at which the

correlations can be assumed equal to one (i.e. the residual time-series are concomitant). For the Mt Stuart wind farm a decomposition to a scale of 64 minutes is appropriate.

The purpose of the wavelet decomposition is to separate turbulent eddies of different spatial and temporal scales. It is expected that larger eddies will affect points that have greater spatial separation. In Figure 1 each dot represents the correlation between wavelet series. For example it is seen that for turbines separated by greater than 200 m the correlation at a scale of 2 minutes is near zero, and the correlation is well described using a log-linear function for distances less than 200 m.

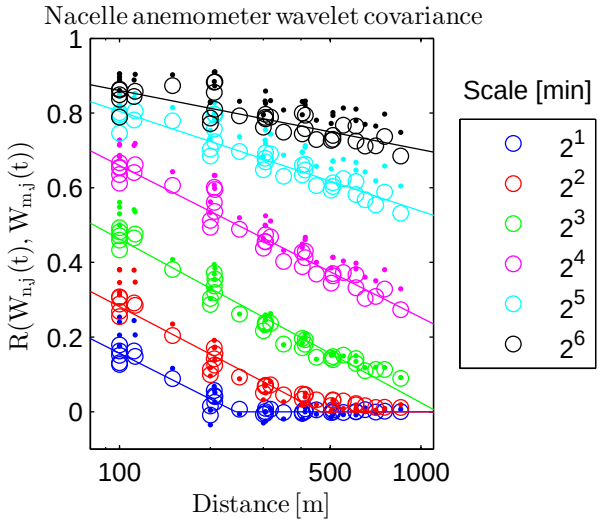

Fig. 1. Wavelet covariance

To be treated as an ARMA process the wavelet series must be transformed to stationary Gaussian processes. It is found that the magnitude of the wavelets are related to the magnitude of the residual time-series thus a Taylor transform, as shown in Equation 10, is applied. The Taylor co-efficients are found using an optimisation search so that the correlation between the transformed wavelet series coefficients and the residual time-series equals zero. The resulting Taylor transformed wavelet series are observed to be non-Gaussian, thus a Johnson transform is applied (as shown in Equation 11), the fitting and application of which is achieved through the use of the Johnson Curve Toolbox for Matlab [15]. These transformations may affect the correlation structures of the wavelet-series, hence the distance relationships in Figure 1 are reaffirmed with circles representing the correlations for the Taylor-Johnson transformed wavelet series, note the distance relationships are calculated for $\Psi_n^{(TJ)}$.

$$\Psi_n^{(T)}(j,\tau) = \frac{\Psi(j,\tau)}{\bar{u}(t)^a} \tag{10}$$

Where a is the Taylor exponent, and T represents the Taylor transformed variable.

$$\Psi n^{(TJ)}(j,\tau) = \gamma + \eta\, sinh^{-1}\left(\frac{\Psi_n^{(T)}(j,\tau) - \epsilon}{\lambda}\right) \tag{11}$$

Where J represents the Johnson transformed variable, γ and η are shape parameters, ϵ is the location parameter, and λ is the scale parameter.

The Taylor-Johnson transformed wavelet series from the nacelle anemometers comprise sets of Gaussian processes and these approximated as an AR process. The Box-Jenkins method using correlograms and partial-correlograms identifies the $\Psi_n^{(TJ)}(j)$ series as pure AR processes with a model order (α) 4 [16]. A Correlated Innovation Matrix (CIM) approach is applied, as described in Equation 12, to simulate the wavelet series.

$$\begin{aligned}\Psi_n^{(TJ)}(j,\tau) =& A_\alpha(j)\cdot\Psi_n^{(TJ)}(j,\tau-\alpha)+ \\ & A_{\alpha-1}(j)\cdot\Psi_n^{(TJ)}(j,\tau-(\alpha-1))+\cdots+ \\ & A_1(j)\cdot\Psi_n^{(TJ)}(j,\tau-1)+\zeta\cdot e_t\end{aligned} \tag{12}$$

Where A_α is the AR coefficient of order α, ζ is the CIM loci, and e is the innovation matix.

C. Simulation using MCP and WMA

The MCP and WMA methodologies can be used to simulate a wind speed time series for each wind turbine in a wind farm and these transformed to power using the wind turbine power curve. The wind farm power time-series is generated from the aggregate of the wind turbine power time-series. The wind power time-series for a wind farm can be simulated using the following procedure:

1) The wind speed and direction time series from the meteorological mast are averaged to a 64 minute sampling interval.
2) For each wind direction sector a random speed up is generated. The speed ups are assumed to be normally distributed with the mean and standard deviation calculated from the frequency weighted speed ups determined from the Mt Stuart wind farm data. The speed up is applied to the meteorological mast wind speeds for times when the wind direction is in the sector being iterated. Thus a MCP scaled wind speed time-series is generated for each wind turbine.
3) The MCP scaled wind speed time-series is then scaled appropriately (by a factor of $\sqrt{2^6}$) and placed into the residual time-series portion of the wavelet structure.
4) For each scale 2^1 through 2^6 minutes wavelet series are simulated. These series are generated using the CIM approach, the CIM loci (ζ) are defined using the Cholesky decomposition of the matrix formed using the turbine separation distances and log-linear relationships (as presented in Figure 1). The CIM series are then inverse Johnson and inverse Taylor transformed and the resultant wavelet series appropriated into the wavelet structure. The parameters for the Johnson and Taylor transformations are derived for each scale from the mean values found using the Mt Stuart data.
5) The inverse wavelet transformation is applied to the simulated wavelet structures to find wind speed time series representative of each wind turbine.
6) The wind speed time-series are transformed to power using the wind turbine power curve, and the wind farm

power time-series calculated as the aggregate of the wind turbine power time-series.

V. Gaussian Speed Ups / Low Pass Filter

The Gaussian filter / Sandia and MCP / WMA methods are both numerically intensive. It is desirable for power systems simulations involving tens to hundreds of wind farms that a simpler model is constructed.

A. GSU

In the development of the MCP algorithm it is noted that the distribution of Speed-ups is approximately Gaussian, and indeed this property is drawn upon in the Gaussian filter. However, the Gaussian filter width is not intrinsically defined by parameters typically encountered in wind farm calculations. Hence, it is intuitive to form a wind farm power curve by generalising the MCP expression as presented in Equation 13 where the distribution of speed ups is Gaussian, this is equivalent to the method derived by Norgard [17]. The mean and standard deviation for the speed ups are taken from the frequency weighted average of all speed ups derived in Section MCP.

$$P_S(u) = \int_{q=0}^{1} P(u \cdot S_{\mu_g,\sigma_g}(q)) \tag{13}$$

Where q is probability.

B. LPF

The spatial integration of wind turbines can be modeled using a first order low pass filter as described in Equation 14 and proposed by Madsen in 1984 [18]. The low pass filter constant for the Mt Stuart wind farm is found by minimising the root-mean-square difference in measured and simulated power spectral densities of wind farm power time-series. As the filter is applied to wind speed time-series it is necessary to use an optimisation routine to find the filter constant.

$$u_{\omega'} = F'\{\frac{F(u)}{1 - M\omega}\} \tag{14}$$

Where ω is frequency, F denotes the Fourier transform, F' the inverse Fourier transform, and M is the low pass filter constant.

C. Simulation using GSU / LPF

The simulation of a wind power time-series is achieved by taking the wind speed time-series from the meteorological mast, applying the low pass filter, and subsequently applying the wind farm power curve.

VI. Wind Farm Efficiency

The wind farm power output is lower than the hypothetical power due to a variety of factors including electrical losses, turbine wakes, high wind hysteresis, and operational efficiency.

The electrical losses in the Mt Stuart wind farm are small and thus omitted. Wake losses for Mt Stuart are likewise small due to the turbines being positioned in a single line perpendicular to the prevailing wind direction and so are also omitted.

High wind hysteresis in wind turbines results from turbine shutting down in high wind conditions to prevent damage. The turbines do not restart until the wind speed drops below some lower wind speed threshold. The control of wind turbines in high wind speeds is complex and type specific, and has not been included in simulations. The omission is likely to have only minor consequences as high wind speed conditions are infrequent.

The operational efficiency (often referred to as the availability) describes the ratio of power produced to that which would be produced if all turbines were operating in an unrestricted manner. Turbines may be restricted due to faults or maintenance. The operational efficiency has been calculated using data from the Mt Stuart wind farm; the average operational efficiency for the period being 97%. A Markov Chain (MC) model, as described by Sulaeman [5], is applied to simulate the operational efficiency. The transition matrix is constructed assuming wind turbines can only be either on or off, thus a total of 10 operational states are possible. The MC model is used to generate operational efficiency time-series and these used to adjust the simulated wind farm power time series.

Note that for a wind farm with a small number of wind turbines the relative step change in power output due to turbines being shut down or started is large, and hence the accuracy of the MC model is intrinsic to the accuracy of ramp rate prediction.

VII. Results

Measured data and results from simulations are presented in Figures 2, 3, and 4. Note that the measured data are obtained from metering of the wind farm power output, and are separate to measurements made at turbines, and have not had filtering applied at the point of measurement. The simulation results are coloured accordingly:

- Measured = black,
- Gaussian filter / Sandia = blue,
- MCP / WMA = red,
- GSU / LPF = green.

Figure 2 presents power curves calculated using the method of bins for measurements and simulations. The measured data additionally have dots spaced at percentiles to illustrate the density of observations.

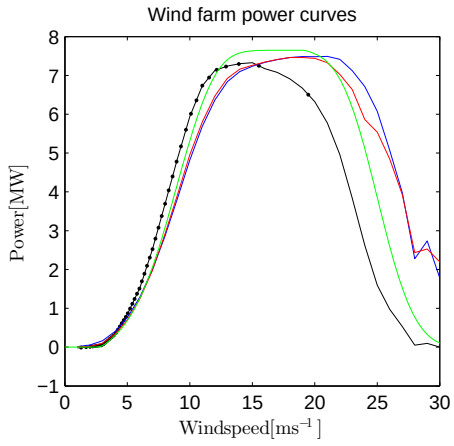

Fig. 2. Power curves

Figure 3 shows cumulative distribution functions. These show the simulated power time-series all slightly under-

estimate the actual power. Note that for low wind speeds (q¡0.2) the Gaussian filter / Sandia method tends to indicate some power production whereas the measured and alternate methods indicate zero power.

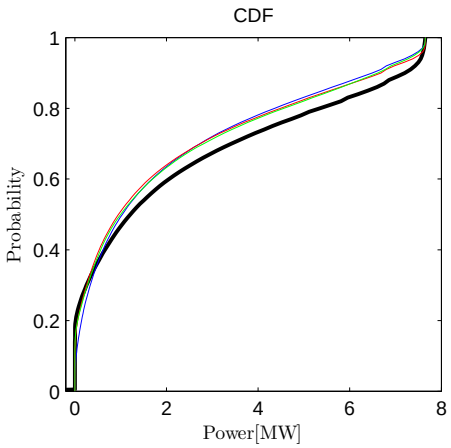

Fig. 3. CDF

Figure 4 presents ramp rates, change in minute to minute power, a critical statistic for estimating reserve requirements (a probability of $1e^{-4}$ corresponds to a once per week event). The observed ramp rates increase faster than log linear, a characteristic that is not well represented by the Gaussian filter / Sandia method. The observed ramps rates better captured by the MCP / WMA method, and the Gaussian speed up / low pass filter matches the measured data very well.

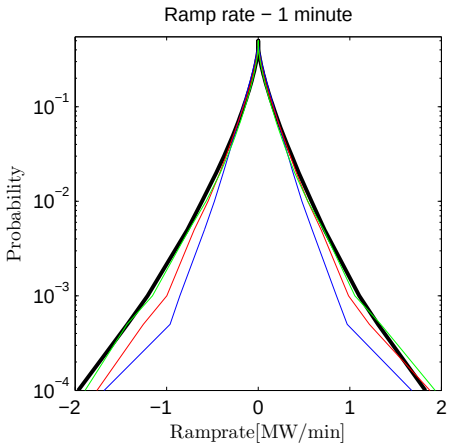

Fig. 4. Ramp rates

VIII. Power curves for differing topographies

The flexibility of the MCP / WMA method enables simulation of power time-series for wind farms of varying topographies. Notional wind farms comprising square arrays of 9, 16, 36, and 64 Gamesa G52 turbines with a spacing of 100 m are developed. The complexity of the terrain is modeled assuming speed ups with standard deviations of 0.01, 0.05, and 0.1 (corresponding to flat, hilly, and steep terrains). Note that wind speed deficit and intra-array turbulence due to turbine wakes are not accounted for.

Model parameters for the GSU / LPF model are fitted to the wind farm power time-series, simulated using the MCP / WMA method, and the results presented in Figure 5. Generation of power time-series is repeated ten times to remove individual sample bias. The solid lines represent σ_g and are are referenced to the left axis. These show the wind farm power curve is smoothed with increases in terrain complexity as well as increases in wind farm size. The low pass filter constant M, is represented using dashed lines, and increases as wind farm size increases. There is little difference in the LPF constant with respect to terrain complexity; unsurprising as the WMA model does not allow for changes in correlation with respect to terrain complexity.

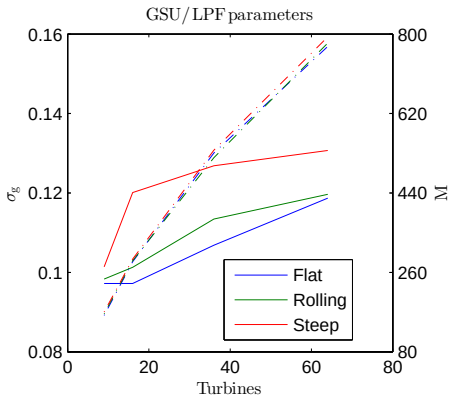

Fig. 5. GSU LPF parameters

IX. Conclusion

The simulation of wind power time-series is essential for determining the effects of integrating wind farms into the power system. The simulation of wind power is derived from measured wind speed time-series and methods to account for the spatial and inertia integration of the wind turbines. Data from the Mt Stuart wind farm has been used to assess the accuracy of simulations developed using the Gaussian filter / Sandia method. It is shown that the Gaussian filter method performs well however is not sufficiently manipulable, and that the inherent assumption of homoskedasticity underestimates ramp rates.

A method using Measure Correlate Predict and Wavelet Multi-Resolution Analysis has been developed and shown to improve results. However, the MCP / WMA method is computationally intensive and not suitable for simulations involving large numbers of wind farms. Hence a simple model using Gaussian Speed-ups and a first order low pass filter is developed and shown to perform well. Relationships between wind farm size, terrain complexity, and GSU / LPF model parameters are developed from power time-series simulated using the MCP / WMA method.

The methods developed here are based on measurements made at a single wind farm. Thus simulations are limited to be representative of wind farms utilising Gamesa G52 wind turbines in rolling hill country. It is posited that wind turbines will provide some smoothing of the wind due to integration over their swept area and inertia; however, no change in PSD evident. This may not be the case for larger wind turbines.

While a Markov chain model has been used to simulate operational efficiency; wake effects have been omitted. While the omission is likely insignificant for the Mt Stuart wind farm, for deep arrays of turbines this may be detrimental.

The analysis in this paper presents methods for simulating dynamic wind power, the results could be further developed using data from more wind farms with different topographies and wind turbine types.

ACKNOWLEDGMENT

This work is part of the GREEN Grid project funded by Ministry Business Innovation and Employment, New Zealand. www.epecentre.ac.nz/greengrid Thanks to Pioneer Generation Limited for the supply of data from the Mt Stuart Wind Farm.

REFERENCES

[1] N. J. Cutler, H. R. Outhred, I. F. MacGill, M. J. Kay, and J. D. Kepert, "Characterizing future large, rapid changes in aggregated wind power using numerical weather prediction spatial fields," *Wind Energy*, vol. 12, no. 6, pp. 542–555, 2009.

[2] IEC, "Wind turbines part 12-1: Power performance measurements of electricity producing wind turbines," 2005.

[3] Gamesa, "Gamesa g52-850 kw," 2007.

[4] G. McNerney and R. Richardson, "The statistical smoothing of power delivered to utilities by multiple wind turbines," *Energy Conversion, IEEE Transactions on*, vol. 7, no. 4, pp. 644–647, 1992.

[5] S. Sulaeman, M. Benidris, and J. Mitra, "A method to model the output power of wind farms in composite system reliability assessment," in *North American Power Symposium (NAPS), 2014*, 2014, pp. 1–6.

[6] R. B. Stull, *An introduction to boundary layer meteorology*, ser. Atmospheric sciences library. Kluwer Academic, 2003, c1988.

[7] L. De Tommasi, M. Gibescu, and A. J. Brand, "A dynamic wind farm aggregate model for the simulation of power fluctuations due to wind turbulence," *Journal of Computational Science*, vol. 1, no. 2, pp. 75–81, 2010.

[8] P. S. Veers, "Three-dimensional wind simulation," in *Eighth ASME Wind Energy Symposium, January 22, 1989 - January 25, 1989*, ser. American Society of Mechanical Engineers, Solar Energy Division (Publication) SED, vol. 7. Publ by American Soc of Mechanical Engineers (ASME), 1988, pp. 23–31.

[9] A. G. Davenport, "The spectrum of horizontal gustiness near the ground in high winds," *Quarterly Journal of the Royal Meteorological Society*, vol. 87, no. 372, pp. 194–211, 1961.

[10] S. Rose and J. Apt, "Generating wind time series as a hybrid of measured and simulated data," *Wind Energy*, vol. 15, no. 5, pp. 699–715, 2012.

[11] T. Nanahara, M. Asari, T. Sato, K. Yamaguchi, M. Shibata, and T. Maejima, "Smoothing effects of distributed wind turbines. part 1. coherence and smoothing effects at a wind farm," *Wind Energy*, vol. 7, no. 2, pp. 61–74, 2004.

[12] A. Derrick, "Development of the measurecorrelatepredict strategy for site assessment," 1993.

[13] A. Llombart, J. M. Fandos, D. Llombart, A. Talayero, and S. J. Watson, "Power curve characterization: Stochastic methods," in *European Wind Energy Conference and Exhibition 2006, EWEC 2006, February 27, 2006 - March 2, 2006*, ser. European Wind Energy Conference and Exhibition 2006, EWEC 2006, vol. 2. European Wind Energy Association, 2006, pp. 1605–1610.

[14] S. Mallat, *A Wavelet Tour of Signal Processing, Third Edition: The Sparse Way*. Academic Press, 2008.

[15] D. L. Jones, "The johnson curve toolbox for matlab: analysis of non-normal data using the johnson system of distributions," 2014.

[16] H. Ltkepohl, *New Introduction to Multiple Time Series Analysis*. Springer, 2007.

[17] N. P and H. H, "A multi-turbine power curve," p. 5, 2004.

[18] W. Schlez, "Voltage fluctuations caused by groups of wind turbines," Doctor of Philiosophy, CREST, 2000.